Insight into the Mechanisms of Cocrystallization of Pharmaceuticals in Supercritical Solvents

ARTICLE *in* CRYSTAL GROWTH & DESIGN · MAY 2015

Impact Factor: 4.89 · DOI: 10.1021/acs.cgd.5b00200

6 AUTHORS, INCLUDING:

Luís Padrela

University of Limerick

13 PUBLICATIONS **180** CITATIONS

SEE PROFILE

Miguel Rodrigues

Technical University of Lisbon

31 PUBLICATIONS **364** CITATIONS

SEE PROFILE

João Miguel Tiago

Technical University of Lisbon

10 PUBLICATIONS **21** CITATIONS

SEE PROFILE

Henrique A Matos

University of Lisbon (Instituto Superior Técnico)

112 PUBLICATIONS **1,367** CITATIONS

SEE PROFILE

CRYSTAL GROWTH & DESIGN

Article

pubs.acs.org/crystal

Insight into the Mechanisms of Cocrystallization of Pharmaceuticals in Supercritical Solvents

Luis Padrela,[§] Miguel A. Rodrigues,*[,§] João Tiago,[§] Sitaram P. Velaga,[⊥] Henrique A. Matos,[§] and Edmundo Gomes de Azevedo[§]

[§]Centro de Química Estrutural and Department of Chemical Engineering, Instituto Superior Técnico, Universidade de Lisboa, Lisboa, Portugal

[⊥]Department of Health Sciences, Luleå University of Technology, 971 87 Luleå, Sweden

Supporting Information

ABSTRACT: Carbon dioxide has been extensively used as a green solvent medium for the crystallization of active pharmaceutical ingredients (APIs) by replacing harmful organic solvents. This work explores the mechanisms underlying a novel recrystallization method—cocrystallization with supercritical solvent (CSS)—which enables APIs cocrystallization by suspending powders in pure CO_2. Six well-known APIs that form cocrystals with saccharin (SAC) were processed by CSS, namely, theophylline (TPL), indomethacin (IND), carbamazepine (CBZ), caffeine (CAF), sulfamethazine (SFZ), and acetylsalicylic acid (ASA). Pure cocrystals were obtained for TPL, IND, and CBZ (with SAC) after 2 h of CSS processing. Convection was revealed to be a determining parameter for successful cocrystallization with high-yield levels. TPL−SAC was selected as a model system to study the cocrystallization kinetics in the gas, supercritical, and liquid phases under different conditions of pressure (8−20 MPa), temperature (30 to 70 °C), and convection regimes. The solubility of each substance in CO_2 was measured at the selected working conditions. TPL−SAC showed a cocrystallization rate of 2.9% min^{-1}, two times higher than that of IND−SAC, due to the higher solubility of TPL in CO_2. The cocrystallization kinetics was also improved by increasing the CO_2 density, showing that cocrystallization was limited by the dissolution of cocrystal formers. Overall, the CSS process has a potential for scale-up as a novel, simple, solvent-free batch process whenever the cocrystal phase is formed in the CO_2 media.

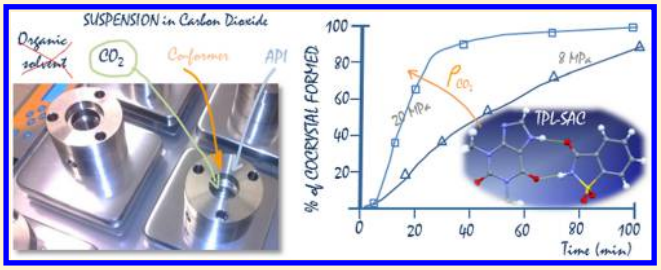

INTRODUCTION

Much work has been published highlighting pharmaceutical cocrystals production and characterization and their potential capacity to tune relevant physical and kinetic properties of drugs.[1−9] Pharmaceutical cocrystals can be prepared by several (classical) methods, namely, mechanochemical (e.g., neat and liquid-assisted grinding) or traditional solution crystallization approaches such as solvent evaporation and slurry techniques.[10,11] However, the use of these traditional techniques may bring undesired problems in the generation of the cocrystal products, such as the generation of amorphous materials when using mechanochemical methods or hydrate/solvate formation, when using solution crystallization methods.

Because of obvious disadvantages presented by classical cocrystal production methods, the development of novel and better methods for screening and production of cocrystals is highly desirable. Supercritical carbon dioxide has been used as an alternative media for crystallization reactions, acting either as a solvent or an antisolvent.[12,13] Supercritical carbon dioxide ($SC\text{-}CO_2$) has been used to induce novel polymorphs, to enable the control of the crystal habit,[14−19] and has more recently also been described as a novel tool for cocrystal engineering.[20−22] Padrela et al.[20] have shown that indomethacin−saccharin cocrystals could be produced either by supercritical antisolvent or by supercritical atomization as straightforward methods, converting crystal clear solutions into micro- to nanosized particles. Additionally, supercritical atomization has shown potential for the generation of novel cocrystal stoichiometries which had not been produced by classical methods.[21] Most interestingly, Padrela et al. [20] observed that a small amount of indomethacin (IND)−saccharin (SAC) cocrystals could be formed when both pure components (IND and SAC) were placed in contact with $SC\text{-}CO_2$. This effect is herein explored as a novel cocrystallization with supercritical solvent (CSS) method that uses the solvent power and the molecular mobility enhancement provided by supercritical fluids, in particular in CO_2, to promote the cocrystallization of an API with a coformer. Previous results suggest that $SC\text{-}CO_2$ has the potential to be a simple (single step), scalable, organic solvent-free alternative for cocrystallization of APIs. To better understand the mechanism of CO_2-mediated cocrystallization and its full potential for industrial

Received: February 9, 2015
Revised: May 6, 2015

DOI: 10.1021/acs.cgd.5b00200
Cryst. Growth Des. XXXX, XXX, XXX−XXX

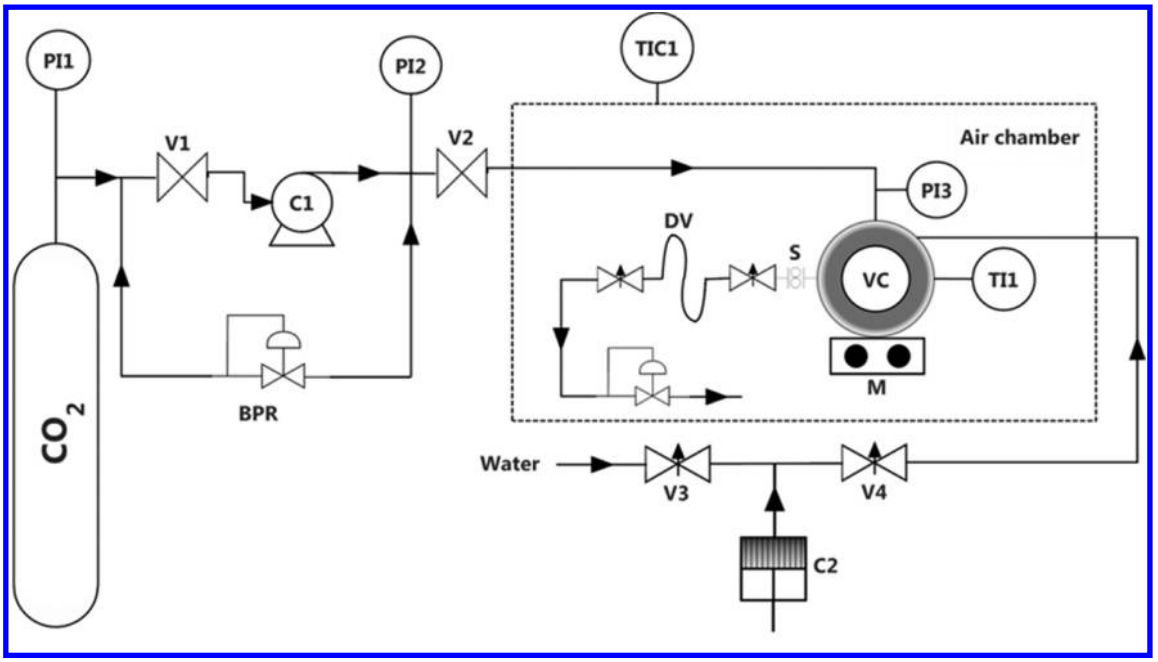

Figure 1. Schematic diagram of the equilibrium solubility apparatus. PI – pressure indicator; V – valve; BPR – back pressure regulator; C – compressor; TI – temperature indicator; TIC – temperature indicator and controller; VC – variable volume high-pressure visual cell; M – magnetic stirrer; S – strainer; DV – dead volume.

application, key issues must be clarified, namely: Is it possible to obtain pure cocrystals by CO_2-mediated cocrystallization? Which systems cocrystallize in CO_2 under what conditions? What is the role of the CO_2 in the cocrystallization?

This work focuses on the action of CO_2 to induce the cocrystallization of six well-known APIs that form cocrystals with SAC: theophylline (TPL), IND, carbamazepine (CBZ), caffeine (CAF), sulfamethazine (SFZ), and acetylsalicylic acid (ASA). We aim to identify limiting parameters (thermodynamic and kinetic) influencing the formation of cocrystals in SC-CO_2. Moreover, some comparative studies were carried out between the use of SC-CO_2, SC-N_2 (which has much smaller solvent power) and supercritical mixtures of CO_2 and ethanol (which have higher solvation capability). We have also measured the cocrystallization rates of the systems IND–SAC and TPL–SAC and the solubilities of the cocrystal formers in CO_2 at corresponding pressure and temperature conditions. Overall, this work should provide some answers for the questions formulated above, thus clarifying the mechanisms underlying cocrystallization in CO_2 and discussing its feasibility as a cocrystallization media.

EXPERIMENTAL SECTION

Materials. Theophylline, IND (γ-form), carbamazepine, acetylsalicylic acid, and saccharin were purchased from Sigma Aldrich (purity of these chemicals was >99.9%). Caffeine was purchased from Fluka (purity > 99.0%) and sulfamethazine from Acros Organics (purity >99.0%). Carbon dioxide (99.98%) was supplied by Air Liquide (Portugal).

Powder X-ray Diffraction (PXRD). X-ray powder data were collected in a D8 Advance Bruker AXS θ–2θ diffractometer, with copper radiation (Cu Kα, λ = 1.5406 Å) and a secondary monochromator. The tube voltage and amperage were 40 kV and 40 mA, respectively. Each sample was scanned with 2θ between 5° and 35° with a step size of 0.02° and 0.5 s at each step. The instrument had previously been calibrated using a silicon standard.

Thermal Analysis. Differential scanning calorimetry (DSC) of the TPL-SAC samples was performed using a differential scanning calorimeter NETZSCH DSC 200 F3 Maia. The samples (6–7 mg) were weighed directly into pierced aluminum pans, on an analytical balance. During the experiments the sample holder was continuously purged with a dry nitrogen flow of 50 mL/min. Nitrogen was used as a purge gas and also as a protective gas. Measurements in the DSC were done using a heating/cooling rate of 10 °C/min.

Determination of the Solubility of APIs and Coformers in CO_2. The APIs and coformers' solubilities in CO_2 were measured using a visual, variable volume high-pressure cell, shown schematically in Figure 1. The visual cell consists of a stainless steel cylinder (with an internal diameter of 24 mm, external diameter of 60 mm, and length of 168 mm) with a high-pressure glass window. This cell is divided into two chambers by a movable stainless steel piston provided with two O-ring seals. The back side of the piston contains the pressuring fluid, water in this case, responsible for moving the piston forward or backward.

Each experimental run started by loading the cell (in the front side of the piston) with 200 mg of the corresponding solid powder and a magnetic stirrer set to 300 rpm. After the cell was closed, the system was pressurized with CO_2, and the air chamber was heated to the desired conditions (see Figure 1). The CO_2 was injected into the cell through valve V2 passing by pressure indicator PI3 where the CO_2 pressure was measured. The water pressure was controlled by moving the piston by changing the pressure of the water in the back of the piston, using the manual compressor C2 (HIP, model 86-6-5). The temperature inside the air chamber was maintained by a digital temperature controller (BTC-9200, ROC). Temperatures were measured with thermocouples (Omega, type T), and the estimated temperature variability was ± 0.1 °C. Pressures in the CO_2 line and in the visual cell were measured with pressure transducers (Setra, model 206) and digital indicators (Setra, model 300D) with an estimated pressure variability of ± 0.01 MPa.

Each test was performed overnight to ensure the equilibrium solubility of solid components, and each point was repeated at least in triplicate and standard deviations were calculated.

At the end of each run, the 14.0 cm^3 (±0.05 cm^3) DV loop was closed, and the visual cell was depressurized. The DV loop tubing was immersed in a liquid nitrogen bath for approximately 30 min to freeze the CO_2. Afterward, the valves that kept the DV loop closed were opened allowing the CO_2 to bubble slowly inside a flask with a known volume of ethanol (for the solubility measurements of IND) or

DOI: 10.1021/acs.cgd.5b00200
Cryst. Growth Des. XXXX, XXX, XXX–XXX

phosphate buffer pH 7.4 (for the solubility measurements of theophylline and saccharin). The solution was used to rinse the DV loop several times and was then analyzed by HPLC or UV spectroscopy. The CO_2 quantity in the DV loop was calculated using its density for the corresponding *P*, *T* conditions.[23]

High-Performance Liquid Chromatography (HPLC). The HPLC procedure for the solubility determination of APIs in CO_2 (presented in detail in the Supporting Information) uses a Jasco HPLC-system apparatus provided with a 3.9 × 150 mm Nova-Pak C18 column (Waters) and equipped with a variable UV detector (set at 254 nm). The column was kept at room temperature. The mobile phase consisted of acetate buffer, pH 4: acetonitrile (95:5), delivered at a flow rate of 1.2 mL min^{-1}. It was filtered through a 0.45 μm membrane and degassed by sonication prior to the use. Elution was isocratic, with a flow rate of 1 mL/min. The injection volume was 20 μL and for the detection a PDA detector was used. An elution time of 12 min sufficed for the analysis of the samples.

A UV spectrophotometer was used wherever HPLC analysis was not feasible. Each sample of IND solution was passed through a 0.20 μm filter and analyzed using an UV spectrophotometer method using microplates. A Spectra max Plus 384 Spectrophotometer was used at a wavelength of 319 nm.

CSS Process Description and Cocrystallization. Figure 2 schematically shows the CSS setup. It consists essentially of an 8 cm^3 stainless steel high-pressure vessel (HPV) with monitorized temperature and pressure using a T-type thermocouple and a pressure transducer (Omega model PX603), respectively. A Newport Compressor (model 46-13421-2) was used to load the CO_2 into a vessel storage cylinder (VSC) before being introduced into the high-pressure vessel. These are placed inside a temperature-controlled air chamber. A total mass of 400 mg of one API (TPL, IND, CBZ, CAF, SFZ, or ASA) and coformer (saccharin) in equimolar amounts (1:1 molar ratio) was inserted in the high-pressure vessel. The two powders were then mixed with CO_2 at 20.0 MPa and 50 °C.

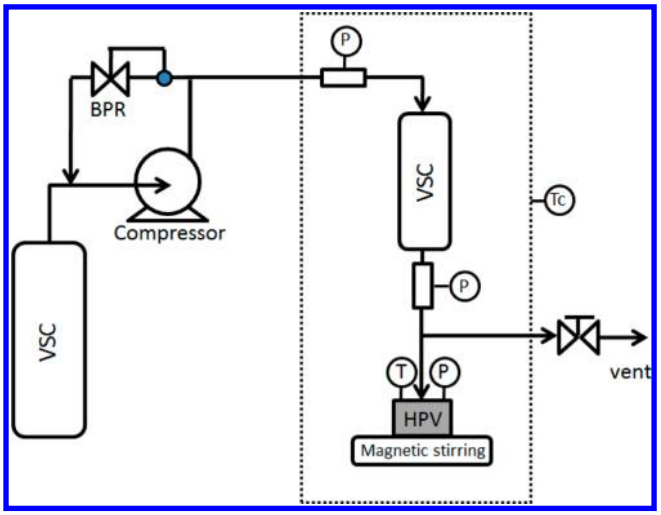

Figure 2. Schematic description of the cocrystallization with supercritical solvent (CSS) setup. VSC − vessel storage cylinder; HPV − high-pressure vessel.

During each experiment, the solid mixture was subjected to magnetic stirring at 300 rpm. After 2 h of reaction, the high-pressure vessel was slowly depressurized and the resulting material was collected. In order to study the effect of convection in the cocrystallization by the CSS technique, some experiments were carried out without magnetic stirring. Negative control experiments were carried without CO_2 (using air at atmospheric pressure) at 50 °C in the CSS apparatus with magnetic stirring. This was important to check the effect of the magnetic stirring alone (without the presence of CO_2).

To evaluate the effect of a different solvent medium in the cocrystallization by the CSS technique, two approaches were used (see Table 1); a total of 1 μL of ethanol per mg of powder was introduced into the high-pressure vessel before the pressurization with CO_2; second, nitrogen (N_2) was also used instead of CO_2 (no ethanol at the conditions mentioned above (20.0 MPa and 50 °C). Note that N_2 is in the supercritical state above 3.40 MPa and −147 °C.).

The material recovered from the experiments was stored in a closed desiccator prior to its characterization.

Cocrystal Formation Kinetics in CSS. Kinetics of TPL−SAC Cocrystal Formation. Cocrystallization of TPL−SAC in the CSS process was monitored using a PXRD quantification method presented in the Supporting Information. As described above, TPL and SAC were introduced in the CSS apparatus, in a 1:1 molar ratio, prior to the pressurization with CO_2. The kinetics of the cocrystallization were analyzed by running the experiments using different reaction times: 0, 5, 20, 30, 45, 60, 90, and 120 min. This was performed under three different conditions: at high density supercritical CO_2 (20.0 MPa, 50 °C), low density supercritical CO_2 (8.0 MPa, 50 °C), and liquid CO_2 (8.0 MPa, 30 °C). The effect of the temperature and CO_2 pressure was also analyzed. It is worth mentioning that a significant amount of experimental work was required to generate all the results: approximately 200 experiments were operated by the CSS technique to complete this task.

Kinetics of IND−SAC Cocrystal Formation. The kinetics of the cocrystallization was studied by running the experiments using different reaction times: 0, 5, 20, 30, 45, 60, 90, and 120 min. This analysis was accomplished using high density supercritical CO_2 (20.0 MPa, 50 °C). The results obtained for the kinetics of IND−SAC cocrystal formation in the CSS technique were analyzed and compared with the kinetics of TPL−SAC cocrystal formation (both processed under the same conditions in supercritical CO_2 for comparison purposes).

Table 1. Evidence from PXRD Analysis for Cocrystallization of Several APIs with SAC after 2 h of Reaction by CSS Technique Using Different Solvent Media at Supercritical Conditions: SC-CO_2, SC-N_2, and SC-CO_2 with ethanol as a Cosolvent (1 μL of EtOH per mg of powder)[a]

	+ saccharin				
	air (0.1 MPa, 50 °C)	SC-CO_2 (20 MPa, 50 °C)	SC-CO_2 (20 MPa, 50 °C)	SC-(CO_2 + EtOH) (20 MPa, 50 °C)	SC-N_2 (20 MPa, 50 °C)
API	300 rpm	not stirred	300 rpm	300 rpm	300 rpm
TPL	− −	+ −	+ +	+ +	+ −
CBZ	− −	+ −	+ +	+ +	+ −
IND	− −	+ −	+ +	+ +	+ −
CAF	− −	− −	− −	− −	+ −
SFZ	− −	− −	− −	+ +	+ −
ASA	− −	− −	− −	− −	− −

[a]Control runs were carried for the stirring effect using static SC-CO_2 (not stirring) and stirring only (without CO_2) in air at normal pressure. − −: mixture of API and saccharin; + −: mixture of cocrystal, API and saccharin; ++: pure cocrystal.

DOI: 10.1021/acs.cgd.5b00200
Cryst. Growth Des. XXXX, XXX, XXX−XXX

RESULTS

Cocrystal Screening by CSS. Table 1 shows the systems studied using the CSS technique. PXRD measurements of the runs using CAF, SFZ, and ASA did not reveal any cocrystal peaks when only CO_2 was used. Instead, the diffractograms obtained matched the mixture of the crystalline forms of both pure components. None of the drugs cocrystallized in air at atmospheric pressure and temperature of 50 °C using only the stirring facility.

Table 1 also shows that cocrystallization was very limited when using CO_2 without stirring, only partial cocrystal formation was observed for the systems TPL−SAC, IND−SAC, and CBZ−SAC, and no cocrystal formation was observed at all (by PXRD) for the remaining systems. However, when using CO_2 with stirring, full cocrystal formation was achieved for TPL−SAC, IND−SAC, and CBZ−SAC. Table 1 also shows that stirring by itself with atmospheric air at 50 °C does not cause cocrystallization of these APIs with SAC.

Figures S1−S6 in the Supporting Information show the PXRD diffractograms for the systems processed in the CSS technique using CO_2 with stirring. The d values and 2θ values of the characteristic PXRD peaks corresponded well with those reported elsewhere.[2,20,21,24,25]

The addition of ethanol as a cosolvent enabled the formation of pure cocrystals of SFZ−SAC, which were never obtained using CO_2 only. Using N_2 instead, the cocrystal was produced with the pure components for all the systems studied except for ASA−SAC.

The effect of stirring is also observed in the DSC thermograms. With magnetic stirring a single melting transition point at 207.2 °C is observed, and not the eutectic melting between 180 and 190 °C (typical when traces of TPL and SAC are present in the mixture). For the experimental run with CO_2 without stirring, a lower eutectic melting at 181.7 °C appears in the DSC curve (Figure 3c), and an additional melting peak at 199 °C is observed. The impurity can also be inferred from the PXRD diffractogram (Figure S1 in the Supporting Information).

Solubility of APIs and Coformers in CO_2. Table 2 shows the measured solubilities of the pure substances TPL, SAC, and IND. As expected, the solubility of each component increases with the CO_2 pressure and temperature. However, compared to TPL and IND, the solubility of SAC is still relatively high in the liquid phase. In supercritical CO_2 (20.0 MPa, 50 °C), SAC is 6 times more soluble than TPL and 10 times more soluble than IND. Table 2 shows that TPL solubility in SC-CO_2 is 9.8×10^{-2} mol m^{-3} (20.0 MPa, 50 °C), which is in agreement with the solubility data reported elsewhere.[26]

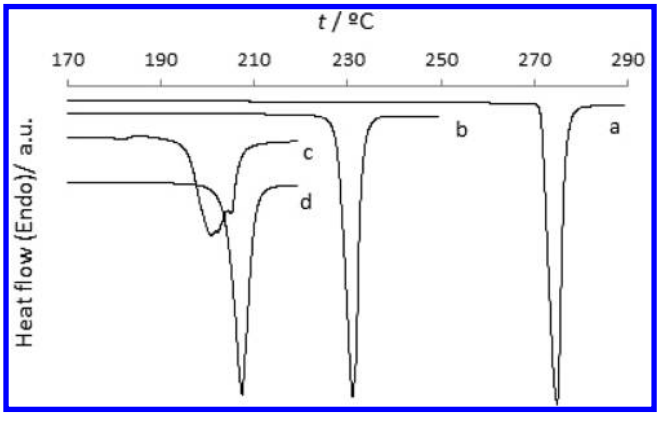

Figure 3. DSC thermograms for (a) pure theophylline, (b) pure saccharin, (c) TPL−SAC cocrystals produced by the CSS process without stirring, and (d) TPL−SAC cocrystals produced by the CSS process with stirring.

Table 2. Solubilities of TPL, SAC, and IND in CO_2 for the Processing Conditions Studied[a]

substance	CO_2 state	pressure (MPa)	temperature (°C)	solubility × 10^2 mol $m^{-3}_{(CO_2)}$
TPL	supercritical	20	50	9.8 ± 1.0
	supercritical	8	50	1.7 ± 0.2
	liquid	8	30	2.7 ± 0.2
SAC	supercritical	20	50	59.2 ± 4.3
	supercritical	8	50	12.2 ± 2.0
	liquid	8	30	22.9 ± 2.7
IND	supercritical	20	50	6.0 ± 0.5
	supercritical	8	50	1.5 ± 0.1
	liquid	8	30	1.1 ± 0.2

[a]TPL − theophylline; SAC − saccharin; IND − indomethacin.

Kinetics of Cocrystal Formation by CSS. The PXRD quantification method developed for TPL−SAC (section SI2 in the Supporting Information) was used to study the cocrystal formation kinetics of TPL−SAC in CO_2. This was prepared for different conditions: SC-CO_2 at high density (20.0 MPa, 50 °C), SC-CO_2 at low density (8.0 MPa, 50 °C), and liquid CO_2 (8.0 MPa, 30 °C).

Figure 4 shows the cocrystallization kinetics for the system TPL−SAC. A two-step linear relation of cocrystallization with time is observed for most of the cocrystallization reaction. An abrupt shift in the slope of the cocrystallization rate is observed at approximately 45 min in liquid CO_2 (8.0 MPa, 30 °C; Figure 4b) and at 30 min in SC-CO_2 (20.0 MPa, 50 °C; Figure 4a). This shift occurred at approximately 80% cocrystallization either for liquid or SC-CO_2. Beyond this point the percentage increased slowly to almost 100% after 2 h of reaction. In the run at 8.0 MPa and 50 °C (Figure 4c), full cocrystallization was still not achieved after 2 h of reaction, and the amount of cocrystal is rather small compared to the other conditions.

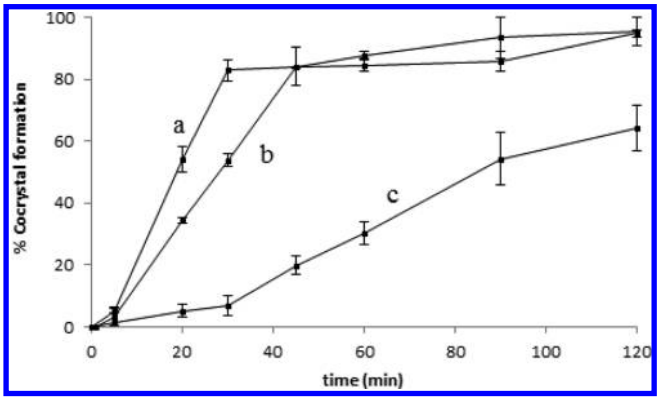

Figure 4. Formation kinetics of TPL−SAC cocrystals in (a) SC-CO_2 at 50 °C and 20.0 MPa, (b) liquid CO_2 at 30 °C and 8.0 MPa, and (c) SC-CO_2 at 50 °C and 8.0 MPa.

Cocrystallization rates were calculated for the linear period. Table 3 presents data generated from the linear regression of the curves from Figure 4a (in the range t = 0−30 min), 3b (t = 0−45 min), and 3c (t = 0−90 min).

DOI: 10.1021/acs.cgd.5b00200
Cryst. Growth Des. XXXX, XXX, XXX−XXX

Table 3. Cocrystallization Rates Observed in Figure 4 and Corresponding Experimental Conditions Operated in the CSS High-Pressure Vessel

					cocrystallization rate × 10^3	
curves	pressure (MPa)	temperature (°C)	CO_2 density × $10^{5\ 23}$ g m^{-3} (state)	TPL solubility × 10^2 mol $m^{-3}(CO_2)$	g min^{-1}	mol·min^{-1} $m^{-3}_{(CO_2)}$
Figure 4a	20	50	7.8 (SC)	9.8 ± 1.0	11.5	0.40
Figure 4b	8	30	7.0 (liq)	2.7 ± 0.2	7.6	0.26
Figure 4c	8	50	2.2 (SC)	1.7 ± 0.2	2.3	0.08

Table 3 shows that cocrystallization in SC-CO_2 at 20.0 MPa and 50 °C (Figure 4a) was nearly 5 times faster than that at 8.0 MPa and 50 °C (Figure 4c). The amount of cocrystal formation per minute was obtained from the slope of each curve represented in Figure 4. The specific cocrystallization rate in SC-CO_2 at 8.0 MPa and 50 °C (Figure 4c) was the smallest. Temperature, pressure, and density all contribute to the cocrystallization rate as will be discussed below.

Pressure and Temperature Effect on TPL−SAC Formation. Several runs were carried on the CSS apparatus for TPL−SAC system at 50 °C and different pressures for 2 h. The results of the pressure effect on cocrystallization are shown in Figure 5.

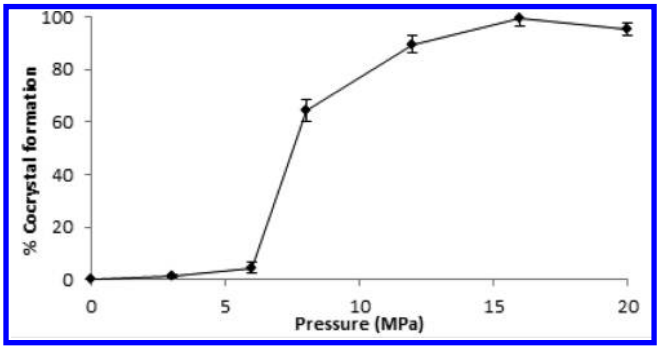

Figure 5. Effect of pressure in the cocrystallization yield (%) of TPL−SAC at 50 °C after 2 h in CO_2.

Above the critical pressure of CO_2 (P_c = 7.38 MPa), there is a noticeable increase in the cocrystal yield after 2 h compared to the runs that used gaseous carbon dioxide (below P_c).

CSS runs (TPL−SAC system and 2 h duration) were carried out for two constant pressure values (at 20.0 and 8.0 MPa) and at different temperatures. Figure 6 shows that the temperature

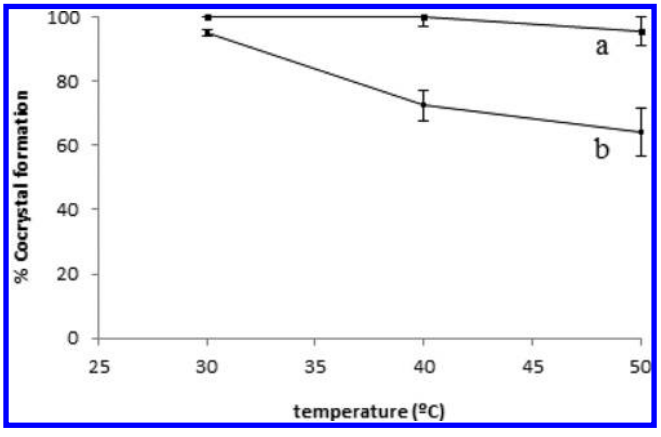

Figure 6. Effect of temperature in the cocrystallization yield (%) of TPL−SAC after 2 h in CO_2 at (a) 20.0 MPa and (b) 8.0 MPa.

slightly decreases the cocrystallization yield. However, it should be borne in mind that a higher temperature at constant pressure implies a smaller quantity of CO_2 due to the decrease in its density.

Figure 6 shows that increasing temperature has a negative impact on the crystallization rate, which could also be explained by the decreasing of CO_2 density.

Kinetics of TPL−SAC versus IND−SAC. The IND−SAC cocrystal formation was performed by the CSS technique at 20.0 MPa and 50 °C and compared with the same conditions used for TPL−SAC kinetic study.

Figure 7 presents the cocrystallization kinetics of TPL−SAC and IND−SAC cocrystals in the CSS technique at 20.0 MPa

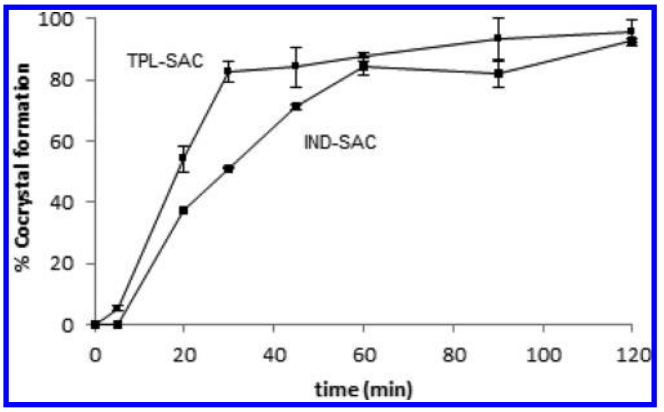

Figure 7. Formation kinetics of TPL−SAC and IND−SAC cocrystals in supercritical CO_2 at 50 °C and 20.0 MPa.

and 50 °C. This shows that IND−SAC formation kinetics is lower than TPL−SAC in supercritical CO_2 at the same conditions of pressure and temperature (20.0 MPa, 50 °C).

Table 4 presents data for the cocrystallization rates calculated for the first linear period of the curves of Figure 7 for TPL−SAC (between t = 0 min and t = 30 min) and IND−SAC (t = 5 min and t = 60 min). The specific cocrystallization rate of TPL−SAC (mol min^{-1} $m^{-3}_{(CO_2)}$) in supercritical carbon dioxide at 20.0 MPa and 50 °C was about 3 times higher than that of IND−SAC.

Table 4. Cocrystallization Rates of TPL−SAC and IND−SAC Cocrystals in the CSS Technique Calculated from Curves of Figure 7

	linear regression		cocrystallization rate	
cocrystal	% $_{(cocrystal)}$ min^{-1}	R^2	10^3 g min^{-1}	10^4 mol min^{-1} $m^{-3}_{(CO_2)}$
TPL−SAC	2.9	0.995	11.5	4.0
IND−SAC	1.5	0.978	6.0	1.4

DOI: 10.1021/acs.cgd.5b00200
Cryst. Growth Des. XXXX, XXX, XXX−XXX

DISCUSSION

Overall, the results show CO_2 acting as a solvent, capable of mediating molecular recognition events, thus enabling or enhancing cocrystallization. Good yields were obtained in half of the cases after 2 h of reaction (Table 1). Albeit the reaction time was relatively short, it proved to be long enough to produce pure cocrystals of the TPL−SAC (Figure 3), IND−SAC, and CBZ−SAC, suggesting that CO_2 may be considered as a serious and very convenient alternative solvent for the production of pure pharmaceutical cocrystals.

The results suggest that cocrystallization is mediated by the dissolution of the substances in CO_2, despite low solubility of the cocrystal components in CO_2 (Table 2). However, the dramatic increase in the cocrystallization observed for conditions beyond the critical point of CO_2 (shown in Figure 5) suggests a possible connection with the solubility issue. Gaseous CO_2 cannot dissolve substances due to its small density, and this ability starts once its critical state is overpassed, even if at a very nearby range. The solvent power increases with the fluids' density, i.e., with either increasing pressure or decreasing temperature. Figures 4−6 show that the kinetics of the cocrystallization follows the density of CO_2. In denser CO_2, the reaction was faster, suggesting that solubility mediates the cocrystallization reaction.

N_2 shows the potential to form cocrystals that are not formed in the presence of CO_2. However, due to the lower density of N_2 (1.9×10^5 g m^{-3}) and possibly low solubility of the pure components, the cocrystallization was small in SC-N_2. Since agitation alone did not promote cocrystallization at atmospheric pressure (Table 1), cocrystallization in N_2 is probably also mediated by a solvation step. The method developed herein to measure solubilities relies on freezing the supercritical phase with liquid N_2, which is not possible when N_2 is the supercritical fluid. Nonetheless, we also observe some cocrystallization when gaseous CO_2 was used (see Figure 5 below critical pressure)—even though its density is 2−3 times smaller than N_2 at 20 MPa and 50 °C. Therefore, considering the relatively high cocrystallization rates observed for supercritical CO_2, it is plausible that a significant drop in solvation power would still enable measurable cocrystallization after 2 h, as observed for N_2 or gaseous CO_2.

The results obtained without stirring (Table 1) show that transport phenomena play an important role in cocrystallization. Without stirring, cocrystallization was significantly limited, which has also been observed previously.[20] In this case, transport from the static powder interface is essentially determined by the solute's diffusivity in the supercritical fluid (on the order of 10^{-8} m^2/s) and the concentration gradient, which is very small due to the component's low solubility. Under such conditions the supercritical phase is unlikely to homogeneously saturate in the reactants, thus hindering cocrystallization. Conversely, stirring promotes intense mass transfer by convection; therefore, cocrystallization becomes not limited by the reactants transport since CO_2 is homogeneously saturated in both components. The saturation of CO_2 is evident in Figure 4, where the cocrystallization curves show a typical zero order reaction, i.e., linear in time. Since CO_2 is always saturated in both components, the reaction velocity is constant. However, an abrupt shift in the linear cocrystallization rate is observed in all cases, which can be explained by two possible reasons:

(1) Some impurities of both TPL and SAC may be deposited in the walls of the apparatus; therefore these impurities are not flowing in the CO_2 with the remaining powder. After most cocrystals are formed (~80% cocrystallization), the absence of TPL and SAC flowing freely in the CO_2 slows down the reaction rate.

(2) Possible differences in the kinetics of dissolution and cocrystallization at the surface and core of the particles may slow down the cocrystallization reaction.

Nonetheless, not all systems cocrystallized in CO_2. For example, although CAF and TPL are both xanthines relatively soluble in CO_2 compared to most APIs, only TPL cocrystallized with SAC. This solvent sensitivity also occurs in the cocrystallization of many APIs with organic solvents. In fact, it is common practice in cocrystallization screenings to use several solvents to increase the chances of successfully obtaining the desired cocrystal. For example, Basavoju et al.[2] cocrystallized IND with SAC in several organic solvents (using solvent evaporation), but when using methanol or acetone a mixture of pure components and cocrystal was obtained instead. The different ability to cocrystallize different APIs using SC-CO_2, SC-CO_2 with ethanol, and N_2 shows that phase equilibria thermodynamics plays an important role as in cocrystallization in liquid organic solvents. This may be related to the dissolved stoichiometric ratio, or to a transition coordination state, required for cocrystallization, which is being hindered in the selected solvent.[27] The overall balance between the affinity of the substances for the solvent or for each other plays an important role herein, as in other processes that are mediated by a solvation step in the supercritical phase, for example, as in the case of impregnation using a supercritical solvent.[28]

Overall, SC-CO_2 showed great potential for production of pharmaceutical cocrystals; however, while trying to control the number of variables in this work, it was possible that only one cocrystal former was used—saccharin—which has a high solubility in CO_2 (10 times higher than TPL or IND). This means that the dissolution of the API (TPL or IND) in the CO_2 is probably the rate-limiting step for the cocrystallization with SAC using the CSS technique. Nonetheless, other coformers less soluble than SAC may cause cocrystallization to be considerably slower, an issue to be clarified in a future work.

The results presented herein make cocrystallization in CO_2 an interesting process for scale-up. In conventional reaction crystallization (in organic solvents), the purification of the cocrystal from the solvent and from other nonreacted pure components could be time and energy expensive. Therefore, the CSS technique is in line with the current process intensification requirements since a considerable capacity for cocrystal formation is herein achieved in a relatively small size reactor and time. Since CSS uses supercritical suspensions rather than solutions, the volume of the crystallization reactor is relatively small if compared even with other SC-CO_2 technologies that require handling supercritical and liquid solutions. Therefore, the volume under pressure, which is usually a deterring factor for scale-up, is herein minimized.

CONCLUSIONS

CO_2 seems to be a "green" and effective cocrystallization media for some APIs. Cocrystals of TPL−SAC, IND−SAC, and CBZ−SAC were produced in approximately 2 h in a CO_2 suspension.

DOI: 10.1021/acs.cgd.5b00200
Cryst. Growth Des. XXXX, XXX, XXX−XXX

Homogeneity in the cocrystallization medium caused by stirring was determinant for a successful cocrystallization most likely due to an enhancement of the intermolecular interactions between the pure components. The use of a cosolvent (ethanol) with CO_2 generated SFZ−SAC cocrystals which could not be produced using CO_2 alone. When using N_2 instead of CO_2, some SFZ−SAC, CAF−SAC cocrystals were also formed as well.

The cocrystallization was revealed to be mediated by a dissolution step: the higher the concentration of the API and coformer in the CO_2 phase, the faster the cocrystallization rate. TPL−SAC showed a higher cocrystallization rate than IND−SAC due to the higher solubility of TPL in CO_2 compared to IND. The cocrystallization followed zero order kinetics, which is explained by the constant saturation of the CO_2 in both cocrystal components.

Overall, CO_2 showed interesting potential for cocrystallization because it enabled reasonably fast kinetics and it is easily separated from the products unlike organic solvents. The proposed new technique of CSS is promising because it reduces the equipment volume and the costs in further solvent separation steps for the production of pharmaceutical cocrystals.

■ ASSOCIATED CONTENT

Supporting Information

High-performance liquid chromatography method for determination of solubility of the APIs in CO_2, PXRD analysis of the samples, and a PXRD method for quantification of TPL−SAC and IND−SAC cocrystals. The Supporting Information is available free of charge on the ACS Publications website at DOI: 10.1021/acs.cgd.5b00200.

■ AUTHOR INFORMATION

Corresponding Author

*E-mail: miguelrodrigues@tecnico.ulisboa.pt.

Notes

The authors declare no competing financial interest.

■ ACKNOWLEDGMENTS

For financial support, the authors are grateful to Fundação para a Ciência e Tecnologia (FCT), Lisbon (Grants SFRH/BD/39836/2007, IF/01183/2013, and Projects PTDC/EQUFTT/099912/2008 and UID/QUI/00100/2013).

■ REFERENCES

(1) Almarsson, Ö.; Zaworotko, M. J. *Chem. Commun.* **2004**, *17*, 1889−1896.
(2) Basavoju, S.; Boström, D.; Velaga, S. *Pharm. Res.* **2008**, *25*, 530−541.
(3) Basavoju, S.; Boström, D.; Velaga, S. *Cryst. Growth Des.* **2006**, *6*, 2699−2708.
(4) Min-Sook, J.; Jeong-Soo, K.; Min-Soo, K.; Alhalaweh, A.; Cho; Wonkyung; Hwang; Sung-Joo; Velaga, S. P. *J. Pharm. Pharmacol.* **2010**, *62*, 1560−1568.
(5) McNamara, D. P.; Childs, S. L.; Giordano, J.; Iarriccio, A.; Cassidy, J.; Shet, M. S.; Mannion, R.; O'Donnell, E.; Park, A. *Pharm. Res.* **2006**, *23*, 1888−1897.
(6) Wuest, J. D. *Nature Chem.* **2012**, *4*, 74−75.
(7) Shan, N.; Zaworotko, M. J. *Drug Discovery Today* **2008**, *13*, 440−446.
(8) Schultheiss, N.; Newman, A. *Cryst. Growth Des.* **2009**, *9*, 2950−2967.
(9) Miroshnyk, I.; Mirza, S.; Sandler, N. *Adv. Drug Delivery Rev.* **2009**, *6*, 333−341.
(10) Weyna, D. R.; Shattock, T.; Vishweshwar, P.; Zaworotko, M. J. *Cryst. Growth Des.* **2009**, *9*, 1106−1123.
(11) Friščić, T.; Jones, W. *Cryst. Growth Des.* **2009**, *9*, 1621−1637.
(12) Uchida, H.; Manaka, A.; Matsuoka, M.; Takiyama, H. *Cryst. Growth Des.* **2004**, *4*, 937−942.
(13) Mazzotti, M.; Fusaro, F.; Muhrer, G. *Cryst. Growth Des.* **2004**, *4*, 881−889.
(14) Bettini, R; Menabeni, R.; Tozzi, R.; Pranzo, M. B.; Pasquali, I.; Chierotti, M. R.; Gobetto, R.; Pellegriono, L. *J. Pharm. Sci.* **2009**, *99*, 1855−1870.
(15) Bettini, R.; Bonassi, L.; Castoro, V.; Rossi, A.; Zema, L.; Gazzaniga, A.; Giordano, F. *Eur. J. Pharm. Sci.* **2001**, *13*, 281−286.
(16) Martín, Á.; Scholle, K.; Mattea, F.; Meterc, D.; Cocero, M. J. *Cryst. Growth Des.* **2009**, *9*, 2504−2511.
(17) Bouchard, A.; Jovanović, N.; Hofland, G. W.; Mendes, E.; Crommelin, D. J. A.; Jiskoot, W.; Witkamp, G.-J. *Cryst. Growth Des.* **2007**, *7*, 1432−1440.
(18) Rodrigues, M.; Padrela, L.; Geraldes, V.; Santos, J.; Matos, H. A.; Azevedo, E. G. *J. Supercrit. Fluids* **2011**, *58*, 303−312.
(19) Roy, C.; Vrel, D.; Veja-González, A.; Jestin, P.; Laugier, S.; Subra-Paternault, P. *J. Supercrit. Fluids* **2011**, *57*, 267−277.
(20) Padrela, L.; Rodrigues, M. A.; Velaga, S. P.; Matos, H. A.; Azevedo, E. G. *Eur. J. Pharm. Sci.* **2009**, *38*, 9−17.
(21) Padrela, L.; Rodrigues, M. A.; Velaga, S. P.; Fernandes, A. C.; Matos, H. A.; Azevedo, E. G. *J. Supercrit. Fluids* **2010**, *53*, 156−164.
(22) Tiago, J. M.; Padrela, L.; Rodrigues, M. A.; Matos, H. A.; Almeida, A. J.; Azevedo, E. G. *Cryst. Growth Des.* **2013**, *13*, 4940−4947.
(23) Linstrom, P. J.,; Mallard, W. G., Eds. *NIST Chemistry WebBook*; NIST Standard Reference Database Number 69; National Institute of Standards and Technology: Gaithersburg, MD, 2005; pp 20899; http://webbook.nist.gov/chemistry.
(24) Lu, E.; Rodríguez-Hornedo, N.; Suryanarayanan, R. *CrystEngComm* **2008**, *10*, 665−668.
(25) Padrela, L.; Azevedo, E. G.; Velaga, S. P. *Drug Dev. Ind. Pharm.* **2012**, *38*, 923−929.
(26) Johannsen, M.; Brunner, G. *Fluid Phase Equilib.* **1994**, *95*, 215−226.
(27) Roy, L.; Lipert, M. P.; Rodríguez-Hornedo N., In *Pharmaceutical Salts and Co-Crystals*; Wouters, J., Thurston, D. E., Eds.; RSC Publishing: London, UK, 2011; Chapter 11, pp 247−276.
(28) Diankov, S.; Barth, D.; Vega-Gonzalez, A.; Pentchev, I.; Subra-Paternault, P. *J. Supercrit. Fluids* **2007**, *41*, 164−172.

DOI: 10.1021/acs.cgd.5b00200
Cryst. Growth Des. XXXX, XXX, XXX−XXX